Ribosome Profiling Reveals Translational Upregulation of Cellular Oxidative Phosphorylation mRNAs During Vaccinia Virus-induced Host Shutoff

Aimei Dai[1*@], Shuai Cao[2*], Pragyesh Dhungel[2*], Yizhao Luan[1], Yizhi Liu[1], Zhi Xie[1#], Zhilong Yang[2#]

1. State Key Lab of Ophthalmology, Guangdong Provincial Key Lab of Ophthalmology and Visual Science, Zhongshan Ophthalmic Center, Sun Yat-sen University, Guangzhou, 500040, China
2. Division of Biology, Kansas State University, Manhattan, Kansas, 66506, USA

Running title: Translational response to VACV infection

To whom correspondence should be addressed. Zhilong Yang, Email: zyang@ksu.edu or Zhi Xie, Email: xiezhi@gmail.com

* Equal contribution. These authors contribute equally to this work and should be regarded as joint first authors.

@Current address: State Key Laboratory of Biocontrol, School of Life Sciences, Sun Yat-sen University, Guangzhou 510275, Guangdong, China.

Word counts

Abstract: 234

Text: 5635

ABSTRACT

Vaccinia virus infection causes a host shutoff, which is marked by global inhibition of host protein synthesis. Though the host shutoff may facilitate reallocation of cellular resources for viral replication and evasion of host anti-viral immune responses, it poses a challenge for continuous synthesis of cellular proteins that are important for viral replication. It is, however, unclear whether and how certain cellular proteins may be selectively synthesized during the vaccinia virus-induced host shutoff. Using simultaneous RNA sequencing and ribosome profiling, two techniques quantifying genome-wide levels of mRNA and active protein translation, respectively, we analyzed the responses of host cells to vaccinia virus infection at both transcriptional and translational levels. The analyses showed that cellular mRNA depletion played a dominant role in the shutoff of host protein synthesis. Though the cellular mRNAs were significantly reduced, relative translation efficiency of a subset of cellular mRNAs increased, particularly those involved in oxidative phosphorylation responsible for cellular energy production. Further experiments demonstrated that the protein levels and activities of oxidative phosphorylation increased during vaccinia virus infection, while inhibition of the cellular oxidative phosphorylation function significantly suppressed vaccinia virus replication. Moreover, short 5' untranslated region of the oxidative phosphorylation mRNAs contributed to the translational upregulation. These results provide evidence of a mechanism that couples translational control and energy metabolism, two processes that all viruses depend on host cells to provide, to support vaccinia virus replication during a host shutoff.

IMPORTANCE

Many viral infections cause global host protein synthesis shutoff. While the host protein synthesis shutoff benefits virus by relocating cellular resources for viral replication, it also poses a challenge to maintain necessary cellular functions for viral replication if continuous protein synthesis is required. Here we measured host mRNA translation rate

Journal of Virology JVI Journal of Virology

during vaccinia virus-induced host shutoff by analyzing total and actively translating mRNAs in a genome-wide manner. The study revealed that oxidative phosphorylation mRNAs were translationally upregulated during vaccinia virus-induced host protein synthesis shutoff. Oxidative phosphorylation is the major cellular energy-producing pathway and we further showed that maintenance of its function was important for vaccinia virus replication. This study highlights that vaccinia virus infection can enhance cellular energy production through translational upregulation in the context of an overall host protein synthesis shutoff to meet energy expenditure.

Journal of Virology JVI Journal of Virology

INTRODUCTION

All viruses depend on their infected host cells for protein synthesis. Many viruses, for example poxviruses, influenza virus, picornavirus and herpesviruses, cause a host shutoff after infection, marked by a global cellular protein synthesis inhibition (1-8). While the host shutoff conserves cellular resources and blunts host antiviral responses that benefit viral replication, it also presents a challenge to maintain the integrity of necessary cellular functions for viral replication, as continuous synthesis of certain host proteins may be needed. However, knowledge is scarce about selectively synthesized cellular proteins and their biological relevance during a virus-induced host shutoff. Determination of selectively synthesized proteins in this process will facilitate identifying cellular functions that are important for viral replication.

Ribosome profiling is a technique based on deep sequencing of ribosome-protected mRNA fragments, providing genome-wide information of mRNAs that are actively translated (9-12). We have previously identified many unexpected translation products of vaccinia virus (VACV) using ribosome profiling (13). Several other studies also identified large numbers of unexpected translation products from human cytomegalovirus (HCMV), coronavirus and Kaposi's sarcoma-associated herpesvirus (KSHV) using ribosome profiling (14-16). Importantly, ribosome profiling can also simultaneously reveal translation of host mRNAs during viral infections. In a recent study, translational changes of host genes upon HCMV infection were studied by simultaneous RNA-Seq and ribosome profiling (17). The study revealed many translationally activated or repressed host genes by HCMV, which does not induce a host shutoff. Given the great sensitivity and resolution, we reasoned that ribosome profiling is a powerful tool to study selectively translated cellular mRNAs by analyzing actively translating and total mRNAs of individual genes during a virus-induced host shutoff.

Poxviruses are a family of large DNA viruses that include highly pathogenic members that infect human and economically important animals, exemplified by the variola virus that causes deadly human disease, smallpox (18). Poxviruses are also developed as

92 agents for cancer therapy and vaccine vector (19, 20). VACV, the prototypic member of
93 poxvirus, was used as the vaccine strain to eradicate smallpox. However, vaccination using
94 VACV may also cause complications such as keratitis, conjunctival disease and iritis in
95 immune compromised individuals (21). It has long been known that VACV rapidly takes
96 over host translational machinery for viral protein synthesis and causes a global host
97 protein synthesis shutoff (4, 5, 22). The shutoff is at least partially attributed to VACV-
98 encoded decapping enzymes, D9 and D10. These decapping enzymes efficiently remove
99 7-methylguanosine caps on the 5' termini of mRNAs (23-28). The decapping renders the
100 mRNAs sensitive to degradation by exonucleases and results in a rapid depletion of
101 mRNAs (24, 25, 29, 30). In addition to mRNA degradation, transcription inhibition may also
102 play a role in this process (31). The global depletion of cellular mRNAs is assumed to
103 contribute to the host shutoff. However, it is largely unknown whether there are cellular
104 proteins selectively translated, and if so, whether those selectively synthesized proteins are
105 important for VACV replication.
106 In this study, we analyzed dynamic transcriptional and translational landscapes of
107 host cells over the course of VACV infection by simultaneous mRNA sequencing (RNA-Seq)
108 and ribosome profiling from VACV- and mock-infected cells. Our study indicated that
109 cellular mRNA depletion played a dominant role in the shutoff of host protein synthesis.
110 Though the cellular mRNA amounts were significantly reduced, relative translation
111 efficiency of a subset of cellular mRNAs increased, particularly for those involved in
112 oxidative phosphorylation responsible for cellular energy production. We further
113 demonstrated that the protein levels and activities of oxidative phosphorylation increased
114 during VACV infection, while inhibition of the oxidative phosphorylation suppressed VACV
115 replication. Short 5' untranslated region (UTR) of the oxidative phosphorylation mRNAs
116 contributed to the translational upregulation. This study revealed that a viral infection
117 enhanced oxidative phosphorylation through translational upregulation in the context of an
118 overall host shutoff.
119

MATERIALS AND METHODS

Cell culture and virus infection

Suspension HeLa S3 cells (ATCC-CCL2.2) were cultured in minimum essential medium (MEM) with spinner modification and 5% equine serum in a 5% CO_2 atmosphere at 37°C. Infection of HeLa S3 cells was carried out as described elsewhere (28). Adhesion HeLa cells (ATCC-CCL2) were cultured in Eagle's Minimum Essential Medium (EMEM) supplemented with 10% fetal bovine serum (FBS). VACV Western Reserve (WR) strain (American Type Culture Collection [ATCC] VR-1354) and WRvFire expressing luciferase under a VACV synthetic early/late promoter were gifts from Dr. Bernard Moss (32). Preparation, titration and infection of VACV were performed as described elsewhere (33).

Antibodies and chemical inhibitors

Anti-MT-CO2, anti-MT-CO1, anti-SDHB, total oxidative phosphorylation human antibody cocktail, and anti-GAPDH antibodies were purchased from Abcam (Cambridge, MA). Anti-tubulin antibody was purchased from Santa Cruz Biotechnology (Dallas, TX). Anti-VACV serum was a gift from Dr. Bernard Moss. Oxidative phosphorylation inhibitors Carbonyl cyanide *m*-chlorophenyl hydrazone (CCCP) and antimycin A were purchased from Sigma-Aldrich (St. Louis, MO). Cytosine arabinoside (AraC) is a VACV DNA replication inhibitor that was also purchased from Sigma-Aldrich.

Ribosome profiling and RNA-Seq

The experiment procedures were described previously (13). Briefly, ribosome profiling was carried out as described elsewhere with minor modifications (10). VACV (at a multiplicity of infection [MOI] of 10)- and mock-infected HeLa S3 cells pretreated with translational inhibitor cycloheximide (CHX) were lysed and treated with DNase (Thermo Fisher Scientific, MA), and the lysate was clarified. Messenger RNA was isolated from a portion of the lysate using oligo(dT) and fragmented using RNaseIII (New England Biolab, MA). The mRNA fragments between 50 and 80 nucleotides (nt) were extracted. The

ribosome-protected RNA fragments (RPFs) were separated by electrophoresis after the lysate was digested with RNase I (Thermo Fisher Scientific), the ribosomes were then isolated by sucrose cushion centrifugation, and the RPFs between 28 and 34 nts were isolated. The purified mRNA and RPFs were used to generate libraries for deep sequencing as described previously (10). The purified libraries were sequenced using a HiSeq 2000 system.

Mapping, quantification and differential gene expression analysis

The adaptors of RNA-Seq and ribosome profiling reads were trimmed using FASTX Toolkit (v0.0.13.2, fastx_clipper: -l 25 –n –v –Q33; fastx_trimmer: -f 1 –Q33). The tRNA and rRNA were removed by Bowtie (v1.0.1, -l 20) (34). The DNA reference sequences coding tRNAs were obtained from the Genomic tRNA Database (http://gtrnadb2009.ucsc.edu/download.html) (35). The DNA reference sequences coding rRNAs were obtained from iGenomes (https://support.illumina.com/sequencing/sequencing_software/igenome.html). The reads were mapped to both the human genome (Ensembl, GRCh37) and the VACV genome (NC_006998.1) using Tophat (v2.0.11, --library-type fr-firststrand) (36). Raw counts of protein-coding genes were quantified by HTSeq (v0.6.1p2) (37). Raw counts of the host genes and the VACV genes were combined and RPKMs (reads per kilobase of transcript per million reads) were calculated by edgeR (38). The raw read numbers were normalized to the effective library sizes of total reads of the host and VACV. Genes with mean RPKM less than 1 were not included for further analysis. The RPKMs of the host genes were used to calculate differentially expressed genes at both mRNA and RPF levels, by comparing expression levels in VACV-infected cells to the mock-infected cells P values from multiple testing were adjusted by Benjamini–Hochberg procedure. Genes with an adjusted P value less than or equal to 0.05 and an absolute value of logarithmic fold changes more than or equal to 2 were identified as differentially expressed.

Relative translation efficiency and Gene Set Enrichment Analysis (GSEA)

Relative translation efficiency (TE) was defined as the ratio of normalized RPF density to normalized mRNA density (17, 39). Differential translation efficiency (DTE) was calculated by the ratio of TE under VACV infected condition to TE under the mock condition. Among genes with a mean log2(RPKM) of four related samples (mRNA and RPF from mock- and VACV-infected cells of each time point) larger than -1, those with a logarithmic value of DTE larger than 1 were defined as translationally upregulated genes, and those with less than -1 were defined as translationally down-regulated genes. GSEA was carried out using the Bioconductor package, “piano” (40).

5’ UTR (untranslated region), 3’ UTR, CDS (coding DNA sequence) and transcript length analysis

Sequences of protein-coding transcripts were obtained from Gencode (v19, http://www.gencodegenes.org/releases/19.html). 5’UTR, CDS, 3’UTR and transcript sequences were extracted from the aforementioned sequences and only the longest isoforms were used for length and minimal free energy (MFE) analyses. The MFE were calculated by the ViennaRNA package (v2.1.8), followed by normalization to sequence length.

Western blotting analysis

Cell lysates were denatured by heating and separated by sodium dodecyl sulphate-polyacrylamide gel electrophoresis, and transferred to a polyvinylidene difluoride membrane for Western blotting analysis following procedure described previously (41).

RNA extraction and quantitative RT-PCR

Total cellular RNA was prepared using Trizol (Thermo Fisher Scientific, MA) according to the manufacturer’s procedure. Total RNA (1 μg) was used for reverse

transcription (RT) using random hexamer. The reverse-transcribed products were used for quantitative PCR of specific genes.

ATP synthase activity assay and ATP level determination.

ATP synthase activities were measured using ATP synthase enzyme activity microplate assay kit (Abcam). Briefly, the samples from mock- or VACV-infected HeLa cells (MOI=5) were collected at different times post-infection. ATP synthase from these samples was immunocaptured within the wells and its enzyme activity was measured by the production of ADP, which is coupled with oxidation of NADH to NAD^+ that is monitored as decrease in absorbance at 340 nm. ATP levels were measured using the ATP determination kit (Molecular Probes™) by a bioluminescence assay using a recombinant firefly luciferase and its substrate luciferin following manufacturer's protocol.

Cell viability assay

HeLa cells were treated with chemicals or solvent vesicle at indicated concentrations. The cells were then trypsinized and resuspended with DMEM after 24 h of treatment, cell suspension was mixed with trypan-blue at the ratio of 1:1 and the cell viability was measured using a LUNA II™ Automated Cell Counter. The data were collected and averaged from at least three independent experiments.

***In vitro* transcription**

RNAs were generated using HiScribe™ T7 High Yield RNA Synthesis Kit (New England Biolab). Briefly, DNA template containing T7 promoter sequence, 5' UTR, firefly or renilla luciferase and poly (A) coding sequences was generated by PCR. *In vitro* transcription and 5' capping with methylated guanine of the RNAs were carried out according to the manufacturer's instructions. The resulted RNAs were purified using Purelink RNA mini Kit (Thermo Fisher Scientific) and quantified for transfection.

RNA transfection and luciferase activity measurement

Equal amounts of firefly luciferase reporter RNA were transfected in Mock- or VACV-infected HeLa cells at 2 h post VACV infection using Lipofectamine 2000 (Thermo Fisher Scientific). Renilla luciferase reporter RNA were cotransfected as internal control of experimental variation. The luciferase activities were measured at 7 h post VACV infection. A Luminometer was used to measure the luciferase activities using appropriate reporter assay reagents (Promega, WI) according to the manufacturer's instructions. Each result was an average of at least three independent experiments.

Detection of newly synthesized proteins.

Newly synthesized proteins were detected using Click-iT® AHA (L-azidohomoalanine) nascent protein kit (Thermo Fisher Scientific) combined with immunoprecipitation of the AHA-labelled proteins. Briefly, culture medium was replaced with methionine-free medium and incubated for 2 h. Then AHA was added to the medium at 100 μM and incubated for 4 h to label nascent proteins. The cells were collected by centrifuging at 1000 g for 5 min and lysed with radio-immunoprecipitation assay (RIPA) lysis buffer at 4 °C for 30 min. Cell lysates were collected by centrifuging at 12,000 g for 10 min at 4 °C, and the proteins in the supernatant were precipitated with methanol and chloroform and resolubilized in 50mM Tris-Cl containing 1% SDS. 200 μg of proteins were subject to click reaction for 30 min to label the AHA-containing peptides with alkyne-biotin using Click-iT® Protein Reaction Buffer Kit according to the manufacture's instruction. The proteins were then precipitated with methanol and chloroform and resolubilized in 50mM Tris-Cl containing 1% SDS and then added equal volume of 50mM Tris-Cl containing 6% NP-40. The AHA-labelled nascent proteins were precipitated using streptavidin beads, eluted and detected using specific antibodies.

Data availability

The sequencing data were deposited at the National Center for Biotechnology Information Sequence Read Archive (accession No: SRP SRP056975 and SRP SRP093314).

RESULTS

Simultaneous RNA-Seq and ribosome profiling in VACV-infected cells

To understand translational regulation and identify selectively translated cellular mRNAs during VACV-induced host shutoff, we carried out simultaneous RNA-Seq and ribosome profiling in VACV- and mock-infected HeLa cells at 2, 4 and 8 hours post infection (hpi) (Fig. 1A). Under these conditions, VACV replication was in the early stage when viral DNA replication did not occur yet at 2 hpi, whereas at 4 hpi and later times VACV replication had proceeded to the post-DNA replication stage (28). RNA-Seq and ribosome profiling quantitatively measured the levels of total mRNA and actively translating mRNAs, respectively (9, 10). We obtained 114.6 to 135.8 millions of reads from individual RNA-Seq samples and 38.0 to 98.7 millions of ribosome protected fragments (RPFs) from individual ribosome profiling samples that were mapped to human and VACV genomes, providing sufficient depth of sequencing reads for further analyses. The analysis of viral mRNA translation from part of the sequencing data was reported elsewhere (13).

Analysis of the cellular RPFs indicated that the ribosome profiling experiments were highly reproducible, evidenced by very strong correlation coefficient ($r>0.98$) of two sets of completely independent ribosome profiling experiments (biological replicates) under the same infection conditions at each time point (Fig. 1B). The high reproducibility of the RNA-Seq and ribosome profiling experiments was also evidenced by strong correlation of the reads from 2, 4 and 8 h of mock-infected cells, where the cells were under the same culture conditions without VACV infection. The correlation coefficients were higher than 0.98 in all the pairwise comparisons of experiments from the three time points (Data not shown). High quality of cellular RPF reads was evidenced by the expected high mapping rates in coding

regions (CDSs) and 5' UTRs, and low mapping rates of 3' UTRs and introns of cellular gene, for both mock-infected (Fig. 1C) and VACV-infected experiments (Fig. 1D). We concluded that the data sets were of high quality and were suitable for systematic analyses.

Messenger RNA depletion plays a dominant role in VACV-induced host shutoff

We first evaluated the contribution of mRNA depletion in VACV-induced host protein synthesis shutoff by analyzing the proportion of cellular RNA reads and RPFs in total reads. The multidimensional scaling plot (MDS) showed a dramatic overall change of cellular mRNA and RPFs at 4 and 8 hpi (Fig. 2A), whereas the change at 2 hpi was subtle compared to mock-infected cells. This finding is consistent with the fact that VACV replication had proceeded to the post-replicative stage at 4 hpi, when the host shutoff occurred. During the host shutoff, the proportion of cellular mRNA reads decreased significantly at 4 and 8 hpi. The cellular RPFs also decreased significantly at 4 and 8 hpi (Fig. 2B). We next characterized the global changes of cellular mRNAs and RPFs in VACV-infected cells versus mock-infected cells at 2, 4 and 8 hpi. Figure 2C shows that the distribution of RPKMs (reads per kilobase of transcript per million reads) of mRNA and RPF reads virtually overlapped in the mock experiments at 2, 4 and 8 hpi. In contrast, the overall RPKMs in VACV-infected cells dramatically decreased after infection, indicating a host shutoff at both transcriptional and translational levels. Because the total cellular and viral mRNA amounts extracted from mock and VACV-infected cells were similar, these results suggested that cellular mRNA depletion was the major contributor of VACV-induced host protein synthesis shutoff.

Relative translation efficiency of host mRNAs during VACV-induced host shutoff

While only a limited number of cellular genes are differentially expressed at 2 hpi, a large number of cellular genes are differentially expressed at 4 and 8 hpi at both mRNA and translation (RPF) levels (Fig. 3A). The differentially expressed genes also overlapped considerably at mRNA and RPF levels, particularly at 4 and 8 hpi (Fig. 3A). Though large

numbers of cellular genes are differentially expressed at 4 and 8 hpi, the majority of them were downregulated, with only a small number of genes upregulated (Fig. 3B and 3C). Since the host cells underwent a global shutoff at both of the mRNA and RPF levels, almost all the cellular functions were downregulated. Here we focused on the genes with increased levels of mRNAs and RPFs because they are the candidates of selectively synthesized genes that are resistant to the general trend of host shutoff. However, GSEA analysis showed no significantly enriched pathways at both mRNA and RPF levels using a cut-off with an adjusted P value <0.05 by Benjamini and Hochberg's false discovery rate (FDR), which was not a surprise due to the global shutoff and only a very limited number of genes being upregulated.

We then employed a relative translation efficiency analysis, which is defined as the ratio of normalized RPFs to mRNA reads (Fig. 3D). It has been shown to be an effective way to identify differentially translated mRNAs in HCMV infection (39). Though the mRNA levels decreased significantly, we observed extensive translation efficiency regulation of cellular mRNAs responding to VACV infection revealed by a large number of mRNAs with differential translation efficiency in VACV- vs. mock-infected cells, particularly at 4 and 8 hpi (Fig. 3E). We hypothesized that the upregulation of the relative translation efficiency of mRNAs can serve as a compensating mechanism to maintain or increase protein levels in the context of decreased mRNA levels. The functions of the involved genes may be important for VACV replication or cell survival. The genes with upregulated relative translation efficiency (>2-fold) were listed in Dataset S1.

To examine this hypothesis, we carried out a GSEA of the host genes that responded to VACV infection with differential relative translation efficiency. Using the same cut-off of the adjusted P value <0.05 by FDR, the GSEA analysis of the genes yielded several enriched pathways with elevated relative translation efficiency, where oxidative phosphorylation was the only enriched function at all the three time points (Fig. 3F), suggesting that it was selectively targeted by translational upregulation in VACV-infected cells.

Oxidative phosphorylation capacity is enhanced during VACV infection, while inhibition of oxidative phosphorylation suppresses VACV replication

Oxidative phosphorylation is the metabolic pathway in which ATP is produced through a series of biochemical reactions in mitochondria. The oxidative phosphorylation genes include over 100 genes that are encoded in both of the nuclear and mitochondrial genomes in mammalian cells. In human cells, the mitochondrial genome encodes 13 proteins that are subunits of oxidative phosphorylation (42, 43). The relative translation efficiency of mRNAs involved in oxidative phosphorylation was increased significantly, while the mRNA levels were decreased at 8 hpi of VACV infection (Fig. 4A and 4B). A heatmap of differential translation efficiency of oxidative phosphorylation mRNAs clearly illustrates translational upregulation for almost all the oxidative phosphorylation genes (Fig. 4C). The RPF levels of a limited number of genes were even increased more than two-fold after VACV infection, which includes 9 out of 13 protein-encoding genes in human mitochondrial genome (Fig. 4D and 2C).

The downregulation of mRNA levels and upregulation of protein levels involved in oxidative phosphorylation were verified by quantitative RT-PCR and Western blotting analysis of nuclear genome-encoded SDHB and mitochondrial genome-encoded MT-CO1 and MT-CO2, which are subunits of the oxidative phosphorylation complexes (Fig. 5A and 5B). To further examine whether oxidative phosphorylation proteins continued to be synthesized during the shutoff after VACV infection, we examined newly synthesized proteins in VACV-infected cells by labelling with AHA using a Click-iT chemistry technique. The newly synthesized proteins were then precipitated and detected using a total oxidative phosphorylation human antibody cocktail that recognizes five proteins of the oxidative phosphorylation complexes. The results indicated increased levels of UQCRC2, SDHB and MT-CO2 in VACV-infected cells comparing to that in mock-infected cells, while the ATP5A level remained stable (or slightly increased) and the NDUFB8 level decreased. The newly synthesized ATP5A, SDHB and MT-CO2 could be clearly detected in VACV-infected cells

369 at higher levels than that in mock-infected cells (Fig. 5C). Interestingly, the NDUFB8 was
370 one of the few oxidative phosphorylation mRNAs with decreased relative translation
371 efficiency at 4 or 8 hpi (Fig. 4C). These findings suggested that some of the mRNAs
372 involved in oxidative phosphorylation were translationally upregulated, which resulted in
373 continuous protein synthesis under the condition of VACV-induced host shutoff.
374 VACV infection has been reported to enhance oxygen consumption rate (44), an
375 indicator of cellular respiration, suggesting that VACV infection may increase oxidative
376 phosphorylation-based ATP production. We in fact observed that the ATP synthase activity
377 and ATP level increased significantly in VACV-infected HeLa cells (Fig. 6A and 6E).
378 Moreover, we tested the effects of Carbonyl cyanide m-chlorophenyl hydrazine (CCCP), an
379 uncoupler of the oxidative phosphorylation, and Antimycin A, an inhibitor of the oxidative
380 phosphorylation complex III, at the concentrations that did not affect cell viability (Fig. 6B).,
381 on VACV replication The addition of both drugs to the culture medium significantly
382 suppressed VACV replication by more than 10-fold (Fig. 6C). Interestingly, CCCP could
383 inhibit VACV replication in a dose-dependent manner (Fig. 6D), which was correlated to a
384 dose-dependent decrease of ATP levels by the CCCP treatment of VACV-infected cells
385 (Fig. 6E). The block of VACV replication by CCCP and Antimycin was at or before late viral
386 protein expression evidenced by a much lower VACV late protein expression in cells
387 treated with CCCP or Antimycin A (Fig. 6F), Further experiment using a reporter VACV
388 containing a firefly luciferase gene under a VACV early/late promoter indicated that both
389 VACV early and late gene expression was affected by CCCP or Antimycin A treatment (Fig.
390 6G and 6H). Because the chemicals were added at 1 hpi, it suggested that the impairment
391 of oxidative phosphorylation started to affect VACV replication at the stage of early gene
392 expression. These results demonstrated that the oxidative phosphorylation function was
393 important for VACV replication, and its ATP generation capacity is enhanced during VACV
394 infection.
395

Short 5' UTRs of oxidative phosphorylation mRNAs can confer a translational advantage in VACV-infected cells

5' UTR plays an important role in regulating mRNA translation (45). We therefore examined whether 5' UTRs may contribute to the upregulation of oxidative phosphorylation mRNA translation efficiency. We did not observe apparent consensus sequences in the 5' UTRs of oxidative phosphorylation mRNAs. Rather, interestingly, we observed that the 5' UTRs of human oxidative phosphorylation mRNAs are shorter compared to the overall mRNAs. The median length of the longest forms of individual 5' UTRs is 102 nts for oxidative phosphorylation mRNAs and 161 nts for the overall mRNAs (Fig. 7A). The minimum free energy (MFE) for RNA folding of the oxidative phosphorylation mRNA 5' UTRs is also significantly higher than that of the overall cellular mRNA 5' UTRs (Fig. 7B), indicating a less complex secondary structure. A shorter 5' UTR with a less complex secondary structure may contribute to the higher translation efficiency of the corresponding mRNAs in VACV-infected cells (46). To test this possibility, we selected four short 5' UTRs from nucleus-derived oxidative phosphorylation mRNAs and generated mRNAs containing individual 5' UTRs upstream of a firefly luciferase reporter gene by *in vitro* transcription. Each of the mRNAs was transfected into uninfected or VACV-infected HeLa cells at 2 hpi together with an RNA containing renilla luciferase reporter gene as transfection efficiency control. Luciferase activities were measured as the indicators of mRNA translation. The use of RNA rather than DNA reporters in this assay ruled out the possibility of difference in luciferase activities attributed to transcription. All the 5' UTRs tested exhibited higher luciferase activities in VACV-infected cells though the enhancement is not linear to the length of the 5' UTRs (Fig. 7C). As a control, a longer 5' UTR (119 nts) of TRIM73 mRNA that is not an oxidative phosphorylation gene did not confer a higher luciferase activity in VACV-infected cells (Fig. 7C). These results suggested that the short oxidative phosphorylation mRNA 5' UTRs can be one mechanism to confer a translational advantage in VACV-infected cells.

To further test whether a shorter 5'UTR may have a translational advantage in VACV-infected cells, we generated another firefly luciferase reporter mRNA containing three tandem copies of COX6A1 5' UTRs. The use of multiple copies of 5' UTRs rather than a longer 5' UTR from another different mRNA was to rule out the contribution of different sequence elements other than the length as much as possible. The mRNA with three copies of 5' UTRs did not exhibit a translational advantage in VACV-infected cells compared to the uninfected cells (Fig. 7D). Interestingly, the luciferase activity of the reporter with the tandem 5' UTR was higher than that with one copy of the COX6A1 5' UTR in uninfected cells (Data not shown), suggesting that the tandem 5' UTR did not downregulate translation of the reporter mRNA in uninfected cells. These experimental results, together with the global analysis, suggested that a short 5' UTR could confer a translational advantage of oxidative phosphorylation mRNAs in VACV-infected cells during the host shutoff. However, it is worth noting that various elements in a 5' UTR can regulate mRNA translation in addition to a short 5' UTR and these results do not exclude other mechanisms.

DISCUSSION

VACV infection causes cellular mRNA degradation. The degradation is through a combined action of VACV-encoded decapping enzymes, D9 and D10, and cellular nuclease XRN1 (23-25, 30). VACV infection also inhibits host cell transcription (31). Our analyses showed that the mRNA depletion plays a major role during the VACV-induced host shutoff that results in similar reduction of ribosome-associated cellular mRNAs. The result is consistent with several previous studies that showed the cellular mRNAs are globally downregulated after poxvirus infections (22, 28, 47-49). However, this does not rule out the possibility that the cellular mRNA translation is also suppressed during VACV infection. In fact, a recent study showed that VACV ORF169 suppresses general cellular protein translation (50). An important question is how some of the cellular mRNAs can escape from the mRNA depletion and translational repression to maintain the integrity of

451 the infected cells at a sufficient level for viral replication. Since the cellular mRNAs and
452 nascent cellular proteins are dramatically downregulated during VACV infection (4, 5, 22,
453 28), measurement of steady-state levels of mRNA and protein during VACV-induced host
454 shutoff may not be able to sensitively identify those selectively expressed genes. Global
455 translation efficiency analysis using simultaneous RNA-Seq and ribosome profiling provides
456 a highly sensitive approach to identify selectively translated mRNAs during a virus-induced
457 host shutoff (11, 39).

458 Oxidative phosphorylation in the mitochondrion is the major source of cellular
459 energy production in the form of ATP (51). Even in cancer cells or rapidly dividing cells in
460 which a higher portion of ATP is produced by substrate phosphorylation during glycolysis in
461 cytoplasm, oxidative phosphorylation is still a major source of ATP production (52). Like all
462 other viruses, VACV replication depends entirely on host cells to provide energy.
463 Interestingly, in the context of a host shutoff, the oxygen consumption rate, an indicator of
464 energy metabolism, increases in VACV-infected cells (44), which may require increased
465 protein expression involved in oxidative phosphorylation through selective protein synthesis.
466 Our analysis of mRNAs with elevated translation efficiency in fact identified oxidative
467 phosphorylation as the primary and consistent target of translation upregulation during
468 VACV infection. Experimental evidence further demonstrated that the oxidative
469 phosphorylation activity is important for VACV replication. Therefore, these data support a
470 model that oxidative phosphorylation mRNA translation is selectively upregulated to meet
471 the energy expenditure when the mRNA levels are reduced during the VACV-induced host
472 shutoff. Our finding is in concert with the notion that VACV infection can reprogram the
473 cellular metabolism to favour viral replication from several recent publications. The study
474 from Fontaine et al. showed that VACV depends more on glutamine rather than glucose for
475 efficient replication (53). While it is possible to produce ATP energy through glycolysis
476 using glucose, a pathway that does not need oxidative phosphorylation, oxidative
477 phosphorylation is required when using glutamine as the cellular fuel. The studies by
478 Mazzon et al. showed that VACV infection increases synthesis of some precursors of

479 cellular energy metabolism utilized in viral replication, which may also require an elevated
480 oxidative phosphorylation capacity (54, 55). Interestingly, a study of protein abundance in
481 VACV-infected cells by mass spectrometry showed that several proteins of oxidative
482 phosphorylation and proton-transporting ATP synthase were among the over-abundant
483 proteins, supporting the conclusion of this study (56).

484 Mitochondrial functions are damaged in many viral infections. For example, HSV-1
485 infection causes degradation of host mitochondrial DNA (57), while Enterovirus 71 and
486 Dengue virus infection causes an oxidative phosphorylation dysfunction in its infected cells
487 (58, 59). On one hand, the disruption of mitochondrial functions may be beneficial for
488 viruses to avoid eliciting innate immune responses. On the other hand, the impairment can
489 hurt the energy production function of mitochondria, on which both the viral replication and
490 cellular survival depend. Impaired oxidative phosphorylation may be able to provide
491 sufficient energy for some viruses. However, for viruses that need a large amount of energy,
492 the impaired oxidative phosphorylation function could be a restriction factor for viral
493 replication. VACV is a large DNA virus that has been annotated to encode over 200 ORFs,
494 with the potential to have additional over 500 non-classical ORFs from our recent analysis
495 of VACV mRNA translation (13, 60). Protein translation is one of the most energy
496 consuming processes that uses 30-40% of all cellular energy (61-63). Compared to many
497 small viruses that encode only one or a few ORFs, translation of the large number of
498 proteins at high levels may need an increased rate of energy production. In fact, it has been
499 shown that the oxygen consumption rate increases during VACV infection (44). The
500 increased ATP synthase activity observed in the present study suggests that at least part of
501 the increased oxygen consumption contributed to ATP production, which is the usable
502 cellular energy source.

503 We in fact have analyzed uORFs, IRES elements and potential conserved
504 sequences in the oxidative phosphorylation mRNA 5' UTRs. However, we did not observe
505 significant differences compared to overall cellular mRNAs. Rather, our analyses suggest
506 that a short, less complex 5' UTR is at least partially responsible for translational

upregulation of some oxidative phosphorylation mRNAs in VACV-infected cells. A short, less complex 5' UTR in *Drosophila* is responsible for higher translation efficiency of some oxidative phosphorylation mRNAs under the condition of dietary restriction (64). Interestingly, the lengths of the VACV 5' UTRs are also short. The 5' UTRs of early mRNAs vary from 3 to 601 nts with a median length of 21 nts, while the 5' UTRs of intermediate and late mRNAs all have a poly(A) leader with a length up to 51 nts (65, 66). As the poly(A) leaders are also short, less complex 5' UTRs, it is possible that both the viral mRNAs and some of the host cellular mRNAs utilize this feature and some common factors for efficient protein synthesis during VACV-induced host shutoff. However, it is unlikely that a short 5' UTR is the only mechanism employed to elevate translation of oxidative phosphorylation mRNAs during the VACV-induced host shutoff. Other sequence characteristics in 5' UTR, CDS or 3' UTR may contribute to the difference. In fact, the CDSs, 3' UTR as well as the full transcripts of oxidative phosphorylation mRNAs are also significantly shorter in length compared to total human cellular mRNAs (Data not shown). These features may also affect other steps of mRNA translation, such as elongation. Again, VACV ORFs encode shorter CDSs compared to cellular ORFs (Data not shown). The 3' UTRs of VACV early mRNAs are generally short, while the 3' UTRs of intermediate and late VACV mRNAs are heterogeneous (65-68). Again, the resemblance of short 5'UTRs, CDSs as wells as the full transcripts of VACV and oxidative phosphorylation mRNAs suggests that they may employ some common strategies for efficient translation during the VACV-induced host shutoff, though the advantages of a shorter 5'UTR, CDS or 3,UTR may provide during this process remain elusive.

While this study showed translation upregulation as a mechanism to enhance the oxidative phosphorylation capability during VACV infection, future studies will be devoted to further understand viral and cellular mechanisms involved in this process. The oxidative phosphorylation in mammals involves more than 100 genes encoded in both nuclear and mitochondrial genomes. Translation of oxidative phosphorylation mRNAs occurs in both cytoplasm and mitochondria using two distinct translation systems. A recent study suggests

that translation in the two organelles is synchronized and the coordination is controlled and initiated by the cytosolic translation (69). The elevation of relative translation efficiency of both mitochondria- and nucleus-encoded oxidative phosphorylation mRNAs during VACV infection supports this notion. However, the translational control of oxidative phosphorylation mRNAs is complex and the mechanism that coordinates their translation in mammalian cells is largely unknown. It has been suggested that the mTORC1 can selectively promote translation of mitochondria-related mRNAs via inhibition of the eukaryotic translation initiation factor 4E-binding proteins (4E-BPs) (70). VACV infection can inhibit 4E-BP1 by stimulating hyper-phosphorylation of 4E-BP1 (71). It is possible that inhibition of 4E-BP1 is partially responsible for the enhancement of oxidative phosphorylation mRNA translation during VACV infection. In addition, while this study addressed the role of protein synthesis in host cell response to VACV infection, we do not exclude other post-translational mechanisms, for example protein stability regulation, in this process.

As host protein synthesis shutoff is caused by infections of many different viruses, selective protein synthesis through translational upregulation during virus-induced host shutoff may be a common mechanism to continuously translate proteins that are important for cells to survive for a sufficient period of time to support viral replication. While this manuscript was under review, another study revealed that the mRNAs important in cell maintenance processes such as oxidative phosphorylation are less affected during influenza virus-induced host shutoff and that is important for viral replication (72). Identification of these selectively translated proteins is important to elucidate the functional relevance and mechanism involved during a virus-induced host shutoff.

ACKNOWLEDGMENT

The authors wish to thank Dr. Bernard Moss (Laboratory of Viral Diseases, National Institutes of Health) for providing materials, reagents and critical comments on the

manuscript. We also thank Dr. Nicholas Wallace (Kansas State University) for helpful comments.

This work was supported by the National Natural Science Foundation of China [31471232], Science and Technology Planning Projects of Guangdong Province [2014B030301040], Joint Research Fund for Overseas Natural Science of China [3030901001222] and Major Program of Science and Technology of Guangzhou [201607020001] to ZX. This work was also supported by grants from National Institutes of Health (AI100919, a subproject of P20GM113117) to ZY. ZY was also supported by the Johnson Cancer Research Center of Kansas State University and NIAID intramural funds. The contents are solely the responsibility of the authors and do not necessarily represent the official views of funding agencies.

REFERENCES

1. **Krausslich HG, Nicklin MJH, Toyoda H, Etchison D, Wimmer E.** 1987. Poliovirus Proteinase-2a Induces Cleavage of Eukaryotic Initiation Factor-4f Polypeptide-P220. J Virol **61:**2711-2718.
2. **Ventoso I, MacMillan SE, Hershey JWB, Carrasco L.** 1998. Poliovirus 2A proteinase cleaves directly the eIF-4G subunit of eIF-4F complex. Febs Lett **435:**79-83.
3. **Katze MG, Krug RM.** 1990. Translational Control in Influenza Virus-Infected Cells. Enzyme **44:**265-277.
4. **Moss B.** 1968. Inhibition of HeLa cell protein synthesis by the vaccinia virion. J Virol **2:**1028-1037.
5. **Moss B, Salzman NP.** 1968. Sequential protein synthesis following vaccinia virus infection. J Virol **2:**1016-1027.
6. **Glaunsinger B, Ganem D.** 2004. Lytic KSHV infection inhibits host gene expression by accelerating global mRNA turnover. Molecular Cell **13:**713-723.

7. **Kwong AD, Frenkel N.** 1987. Herpes-Simplex Virus-Infected Cells Contain a Function(S) That Destabilizes Both Host and Viral Messenger-Rnas. Proc Natl Acad Sci USA **84:**1926-1930.

8. **Fenwick ML, Mcmenamin MM.** 1984. Early Virion-Associated Suppression of Cellular Protein-Synthesis by Herpes-Simplex Virus Is Accompanied by Inactivation of Messenger-Rna. J Gen Virol **65:**1225-1228.

9. **Ingolia NT, Ghaemmaghami S, Newman JR, Weissman JS.** 2009. Genome-wide analysis in vivo of translation with nucleotide resolution using ribosome profiling. Science **324:**218-223.

10. **Ingolia NT, Lareau LF, Weissman JS.** 2011. Ribosome profiling of mouse embryonic stem cells reveals the complexity and dynamics of mammalian proteomes. Cell **147:**789-802.

11. **Ingolia NT.** 2014. Ribosome profiling: new views of translation, from single codons to genome scale. Nat Rev Genet **15:**205-213.

12. **Xie SQ, Nie P, Wang Y, Wang H, Li H, Yang Z, Liu Y, Ren J, Xie Z.** 2016. RPFdb: a database for genome wide information of translated mRNA generated from ribosome profiling. Nucleic Acids Res **44:**D254-258.

13. **Yang Z, Cao S, Martens CA, Porcella SF, Xie Z, Ma M, Shen B, Moss B.** 2015. Deciphering poxvirus gene expression by RNA sequencing and ribosome profiling. J Virol **89:**6874-6886.

14. **Stern-Ginossar N, Weisburd B, Michalski A, Le VT, Hein MY, Huang SX, Ma M, Shen B, Qian SB, Hengel H, Mann M, Ingolia NT, Weissman JS.** 2012. Decoding human cytomegalovirus. Science **338:**1088-1093.

15. **Arias C, Weisburd B, Stern-Ginossar N, Mercier A, Madrid AS, Bellare P, Holdorf M, Weissman JS, Ganem D.** 2014. KSHV 2.0: a comprehensive annotation of the Kaposi's sarcoma-associated herpesvirus genome using next-generation sequencing reveals novel genomic and functional features. PLoS Pathog **10:**e1003847.

16. **Irigoyen N, Firth AE, Jones JD, Chung BY, Siddell SG, Brierley I.** 2016. High-Resolution Analysis of Coronavirus Gene Expression by RNA Sequencing and Ribosome Profiling. PLoS Pathog **12:**e1005473.

17. **Tirosh O, Cohen Y, Shitrit A, Shani O, Le-Trilling VT, Trilling M, Friedlander G, Tanenbaum M, Stern-Ginossar N.** 2015. The Transcription and Translation Landscapes during Human Cytomegalovirus Infection Reveal Novel Host-Pathogen Interactions. PLoS Pathog **11:**e1005288.

18. **Moss B.** 2013. Poxviridae: The viruses and their replication. Fields Virology, eds, Knipe DM, Howley PM **2:**2129-2159.

19. **Moss B.** 2013. Reflections on the early development of poxvirus vectors. Vaccine **31:**4220-4222.

20. **Chan WM, McFadden G.** 2014. Oncolytic Poxviruses. Annual Review of Virology, Vol 1 **1:**191-214.

21. **Pepose JS, Margolis TP, LaRussa P, Pavan-Langston D.** 2003. Ocular complications of smallpox vaccination. Am J Ophthalmol **136:**343-352.

22. **Becker Y, Joklik WK.** 1964. Messenger Rna in Cells Infected with Vaccinia Virus. Proc Natl Acad Sci U S A **51:**577-585.

23. **Parrish S, Moss B.** 2006. Characterization of a vaccinia virus mutant with a deletion of the D10R gene encoding a putative negative regulator of gene expression. J Virol **80:**553-561.

24. **Parrish S, Moss B.** 2007. Characterization of a second vaccinia virus mRNA-decapping enzyme conserved in poxviruses. J Virol **81:**12973-12978.

25. **Parrish S, Resch W, Moss B.** 2007. Vaccinia virus D10 protein has mRNA decapping activity, providing a mechanism for control of host and viral gene expression. Proc Natl Acad Sci U S A **104:**2139-2144.

26. **Liu SW, Wyatt LS, Orandle MS, Minai M, Moss B.** 2014. The D10 decapping enzyme of vaccinia virus contributes to decay of cellular and viral mRNAs and to virulence in mice. J Virol **88:**202-211.

27. **Shors T, Keck JG, Moss B.** 1999. Down regulation of gene expression by the vaccinia virus D10 protein. J Virol **73:**791-796.

28. **Yang Z, Bruno DP, Martens CA, Porcella SF, Moss B.** 2010. Simultaneous high-resolution analysis of vaccinia virus and host cell transcriptomes by deep RNA sequencing. Proc Natl Acad Sci U S A **107:**11513-11518.

29. **Lewis JD, Izaurralde E.** 1997. The role of the cap structure in RNA processing and nuclear export. Eur J Biochem **247:**461-469.

30. **Burgess HM, Mohr I.** 2015. Cellular 5 '-3 ' mRNA Exonuclease Xrn1 Controls Double-Stranded RNA Accumulation and Anti-Viral Responses. Cell Host & Microbe **17:**332-344.

31. **Pedley S, Cooper RJ.** 1984. The inhibition of HeLa cell RNA synthesis following infection with vaccinia virus. J Gen Virol **65 (Pt 10):**1687-1697.

32. **Townsley AC, Weisberg AS, Wagenaar TR, Moss B.** 2006. Vaccinia virus entry into cells via a low-pH-dependent endosomal pathway. J Virol **80:**8899-8908.

33. **Earl PL, Cooper N, Wyatt LS, Moss B, Carroll MW.** 2001. Preparation of cell cultures and vaccinia virus stocks. Curr Protoc Mol Biol **Chapter 16:**Unit16 16.

34. **Langmead B, Trapnell C, Pop M, Salzberg SL.** 2009. Ultrafast and memory-efficient alignment of short DNA sequences to the human genome. Genome Biol **10:**R25.

35. **Chan PP, Lowe TM.** 2009. GtRNAdb: a database of transfer RNA genes detected in genomic sequence. Nucleic Acids Res **37:**D93-97.

36. **Trapnell C, Pachter L, Salzberg SL.** 2009. TopHat: discovering splice junctions with RNA-Seq. Bioinformatics **25:**1105-1111.

37. **Anders S, Pyl PT, Huber W.** 2015. HTSeq--a Python framework to work with high-throughput sequencing data. Bioinformatics **31:**166-169.

38. **Robinson MD, McCarthy DJ, Smyth GK.** 2010. edgeR: a Bioconductor package for differential expression analysis of digital gene expression data. Bioinformatics **26:**139-140.

673 39. **Stern-Ginossar N.** 2015. Decoding viral infection by ribosome profiling. J Virol
674 **89:**6164-6166.
675 40. **Varemo L, Nielsen J, Nookaew I.** 2013. Enriching the gene set analysis of
676 genome-wide data by incorporating directionality of gene expression and combining
677 statistical hypotheses and methods. Nucleic Acids Res **41:**4378-4391.
678 41. **Yang Z, Moss B.** 2009. Interaction of the vaccinia virus RNA polymerase-
679 associated 94-kilodalton protein with the early transcription factor. J Virol **83:**12018-
680 12026.
681 42. **Smeitink J, van den Heuvel L, DiMauro S.** 2001. The genetics and pathology of
682 oxidative phosphorylation. Nat Rev Genet **2:**342-352.
683 43. **Taanman JW.** 1999. The mitochondrial genome: structure, transcription, translation
684 and replication. Biochim Biophys Acta **1410:**103-123.
685 44. **Greseth MD, Traktman P.** 2014. De novo fatty acid biosynthesis contributes
686 significantly to establishment of a bioenergetically favorable environment for
687 vaccinia virus infection. PLoS Pathog **10:**e1004021.
688 45. **Araujo PR, Yoon K, Ko D, Smith AD, Qiao M, Suresh U, Burns SC, Penalva LO.**
689 2012. Before It Gets Started: Regulating Translation at the 5' UTR. Comp Funct
690 Genomics **2012:**475731.
691 46. **Cenik C, Derti A, Mellor JC, Berriz GF, Roth FP.** 2010. Genome-wide functional
692 analysis of human 5' untranslated region introns. Genome Biol **11:**R29.
693 47. **Guerra S, Lopez-Fernandez LA, Pascual-Montano A, Munoz M, Harshman K,**
694 **Esteban M.** 2003. Cellular gene expression survey of vaccinia virus infection of
695 human HeLa cells. J Virol **77:**6493-6506.
696 48. **Boone RF, Moss B.** 1978. Sequence complexity and relative abundance of
697 vaccinia virus mRNA's synthesized in vivo and in vitro. J Virol **26:**554-569.
698 49. **Brum LM, Lopez MC, Varela JC, Baker HV, Moyer RW.** 2003. Microarray analysis
699 of A549 cells infected with rabbitpox virus (RPV): a comparison of wild-type RPV
700 and RPV deleted for the host range gene, SPI-1. Virology **315:**322-334.

50. **Strnadova P, Ren H, Valentine R, Mazzon M, Sweeney TR, Brierley I, Smith GL.** 2015. Inhibition of Translation Initiation by Protein 169: A Vaccinia Virus Strategy to Suppress Innate and Adaptive Immunity and Alter Virus Virulence. PLoS Pathog **11:**e1005151.

51. **Mitchell P, Moyle J.** 1967. Chemiosmotic Hypothesis of Oxidative Phosphorylation. Nature **213:**137-&.

52. **Cairns RA, Harris IS, Mak TW.** 2011. Regulation of cancer cell metabolism. Nature Reviews Cancer **11:**85-95.

53. **Fontaine KA, Camarda R, Lagunoff M.** 2014. Vaccinia virus requires glutamine but not glucose for efficient replication. J Virol **88:**4366-4374.

54. **Mazzon M, Castro C, Roberts LD, Griffin JL, Smith GL.** 2015. A role for vaccinia virus protein C16 in reprogramming cellular energy metabolism. J Gen Virol **96:**395-407.

55. **Mazzon M, Peters NE, Loenarz C, Krysztofinska EM, Ember SW, Ferguson BJ, Smith GL.** 2013. A mechanism for induction of a hypoxic response by vaccinia virus. Proc Natl Acad Sci U S A **110:**12444-12449.

56. **Chou W, Ngo T, Gershon PD.** 2012. An overview of the vaccinia virus infectome: a survey of the proteins of the poxvirus-infected cell. J Virol **86:**1487-1499.

57. **Saffran HA, Pare JM, Corcoran JA, Weller SK, Smiley JR.** 2007. Herpes simplex virus eliminates host mitochondrial DNA. EMBO Rep **8:**188-193.

58. **El-Bacha T, Midlej V, Pereira da Silva AP, Silva da Costa L, Benchimol M, Galina A, Da Poian AT.** 2007. Mitochondrial and bioenergetic dysfunction in human hepatic cells infected with dengue 2 virus. Biochim Biophys Acta **1772:**1158-1166.

59. **Cheng ML, Weng SF, Kuo CH, Ho HY.** 2014. Enterovirus 71 induces mitochondrial reactive oxygen species generation that is required for efficient replication. PLoS One **9:**e113234.

60. **Yang Z, Moss B.** 2015. Decoding poxvirus genome. Oncotarget **6:**28513-28514.

61. **Topisirovic I, Sonenberg N.** 2011. mRNA translation and energy metabolism in cancer: the role of the MAPK and mTORC1 pathways. Cold Spring Harb Symp Quant Biol **76:**355-367.

62. **Buttgereit F, Brand MD.** 1995. A hierarchy of ATP-consuming processes in mammalian cells. Biochem J **312 (Pt 1):**163-167.

63. **Rolfe DF, Brown GC.** 1997. Cellular energy utilization and molecular origin of standard metabolic rate in mammals. Physiol Rev **77:**731-758.

64. **Zid BM, Rogers AN, Katewa SD, Vargas MA, Kolipinski MC, Lu TA, Benzer S, Kapahi P.** 2009. 4E-BP extends lifespan upon dietary restriction by enhancing mitochondrial activity in Drosophila. Cell **139:**149-160.

65. **Yang Z, Bruno DP, Martens CA, Porcella SF, Moss B.** 2011. Genome-wide analysis of the 5' and 3' ends of vaccinia virus early mRNAs delineates regulatory sequences of annotated and anomalous transcripts. J Virol **85:**5897-5909.

66. **Yang Z, Martens CA, Bruno DP, Porcella SF, Moss B.** 2012. Pervasive initiation and 3'-end formation of poxvirus postreplicative RNAs. J Biol Chem **287:**31050-31060.

67. **Cooper JA, Wittek R, Moss B.** 1981. Extension of the transcriptional and translational map of the left end of the vaccinia virus genome to 21 kilobase pairs. J Virol **39:**733-745.

68. **Mahr A, Roberts BE.** 1984. Arrangement of late RNAs transcribed from a 7.1-kilobase EcoRI vaccinia virus DNA fragment. J Virol **49:**510-520.

69. **Couvillion MT, Soto IC, Shipkovenska G, Churchman LS.** 2016. Synchronized mitochondrial and cytosolic translation programs. Nature **533:**499-503.

70. **Morita M, Gravel SP, Chenard V, Sikstrom K, Zheng L, Alain T, Gandin V, Avizonis D, Arguello M, Zakaria C, McLaughlan S, Nouet Y, Pause A, Pollak M, Gottlieb E, Larsson O, St-Pierre J, Topisirovic I, Sonenberg N.** 2013. mTORC1 controls mitochondrial activity and biogenesis through 4E-BP-dependent translational regulation. Cell Metab **18:**698-711.

71. **Walsh D, Arias C, Perez C, Halladin D, Escandon M, Ueda T, Watanabe-Fukunaga R, Fukunaga R, Mohr I.** 2008. Eukaryotic translation initiation factor 4F architectural alterations accompany translation initiation factor redistribution in poxvirus-infected cells. Mol Cell Biol **28:**2648-2658.

72. **Bercovich-Kinori A, Tai J, Gelbart IA, Shitrit A, Ben-Moshe S, Drori Y, Itzkovitz S, Mandelboim M, Stern-Ginossar N.** 2016. A systematic view on influenza induced host shutoff. Elife **5**.

765 **FIGURE LEGENDS**

766

767 **Fig 1. Experimental approach for simultaneous RNA-Seq and ribosome profiling**
768 **during VACV infection.** (A) Overall experimental design. HeLa S3 cells were mock- or
769 VACV-infected and harvested at 2, 4, and 8 hpi, followed by RNA-Seq and ribosome
770 profiling. (B) High reproducibility of the ribosome profiling experiments. Correlation analysis
771 of cellular reads between ribosome profiling experiments of two biological replicates under
772 VACV-infected condition at 2, 4 and 8 hpi, with Pearson's correlation coefficient shown.
773 RPKM: Reads Per Kilobase of transcript per Million mapped reads. (C, D) Reads density
774 (number of mapped reads divided by length) on genomic regions of 5' UTRs, CDSs, 3'
775 UTRs and introns of cellular mRNAs are shown. The mRNAs are in green and RPFs are in
776 red, under mock condition (C) and VACV-infected condition (D), respectively.

777
778 **Fig 2. Global analysis of mRNA and RPF reads reveals the characteristics of VACV-**
779 **induced host shutoff.** (A) Multidimensional scaling (MDS) plot of Ribo-seq and RNA-seq
780 datasets is used to plot the sample relationship. The log2 fold changes of the most variable
781 500 genes between samples of Ribo-seq and RNA-seq datasets were approximated. The
782 dimension 1 and dimension 2 of the MDS plot were presented, where dimension 1 explains
783 87.45% of variability and dimension explains 6.83% of variability. (B) Mapping efficiency of
784 mRNA/RPF reads of human (black) and VACV (white) genomes at 2, 4 and 8 hpi. (C)
785 Cumulative distribution of gene expression at mRNA (upper panel) and RPF (bottom panel)
786 levels, with time points shown in different colors.

787
788 **Fig. 3. Differential mRNA, RPF and relative translation efficiency analyses of cellular**
789 **genes during VACV infection.** (A) Venn diagram of numbers of differentially expressed
790 genes (DEGs, p.adj <= 0.05 and absolute value of log2FoldChange >= 2) present at mRNA
791 and RPF levels at 2, 4 and 8 hpi. (B, C) Volcano plots of mRNA (B) and RPF (C) levels,
792 with differentially expressed genes (DEGs) shown in red points and mitochondrial (MT)
793 genes shown in blue circles. (D) Relative translation efficiency (TE) is defined as the ratio

of normalized ribosome protected fragments to normalized mRNA reads density on CDS region. (E) Scatter plot of mean value log2(RPKM) (μ) under mock and VACV-infected conditions of mRNA/RPF reads, versus logarithmic value of difference of TE under VACV-infected condition to that under mock condition (log2DTE). Translationally upregulated cellular genes (log2DTE >= 1 and μ >= -1) are shown in red and downregulated genes (log2DTE <= -1 and μ >= -1) are shown in blue. Mitochondrial genes are highlighted in green. Numbers of up/down-regulated genes are also shown. (F) Gene Set Enrichment Analysis (GSEA) of genes with upregulated translation efficiency using the KEGG pathway dataset. P values were adjusted for multiple testing using FDR. NS: not significant, where adjusted P value > 0.05.

Fig 4. Oxidative phosphorylation genes are enriched in mRNAs with enhanced relative translation efficiency. (A, B) Boxplots of oxidative phosphorylation genes (red), and other cellular genes (white) at the DTE levels (A) and mRNA levels (B). *** indicates p < 0.001 using Mann-Whitney U test. (C) Heatmap of DTE of oxidative phosphorylation genes at 2, 4 and 8 hpi. (D) Heatmap of cellular genes with increased RPFs (more than 4-fold) at 2, 4 or 8 h post VACV infection. FC, Fold Change.

Fig 5. Increased synthesis of oxidative phosphorylation proteins during VACV-induced host shutoff. (A) Western blotting analyses of SDHB, MT-CO1 and MT-CO2 levels during the course of VACV infection (MOI=5). Beta-Tubulin or GAPDH were used as loading controls. A representative of at least three independent experiments is displayed. (B) Quantitative RT-PCR analyses of mRNA levels of SDHB, MT-CO1 and MT-CO2 genes. The mRNA levels were normalized to 18S rRNA levels at different time points. Each result is an average of at least three independent experiments. The error bars indicate standard deviation of three experiments. (C) HeLa cells infected with VACV (MOI=5) or mock-infected were starved in methionine-free media and then incubated in media-containing AHA between 3 and 7 hpi. Total proteins (left) and newly synthesized proteins labelled with AHA-containing peptides with alkyne-biotin (right) that were precipitated by streptavidin

beads were subjected to Western blotting analyses using a total oxidative phosphorylation human antibody cocktail. M: mock infection; I: infection.

Fig. 6. Oxidative phosphorylation activity plays an important role in VACV infection (A) ATP synthase activity is enhanced in VACV-infected HeLa cells. HeLa cells were infected with VACV at an MOI of 3 and the ATP synthase activities were determined at 2, 8 and 24 hpi. ATP synthase activities were measured using ATP synthase enzyme activity microplate assay kit. Significant differences defined by a P value <0.05 are indicated by asterisks. (B) HeLa cells were treated with indicated chemicals (CCCP (1 μM) and Antimycin A (20 μM)) and the cell viabilities were determined at 24 h post treatment. (C) Inhibition of VACV replication by mitochondrial function inhibitors CCCP (1 μM) and Antimycin A (20 μM). HeLa cells were infected with VACV at an MOI of 3. The indicated chemicals were added in media at 1 hpi. VACV titers were determined at 24 hpi by a plaque assay. Significant differences defined by a P value <0.05 are indicated by asterisks. (D) HeLa cells infected with VACV were treated with CCCP at indicated concentrations that did not significantly affect cell viability (not shown). VACV titers were determined by a plaque assay 24 hpi. Significant differences to the titer with no CCCP treatment defined by a P value <0.05 are indicated by asterisks. (E) ATP levels of uninfected HeLa cells (Un) or HeLa cells infected with VACV were treated with indicated concentrations of CCCP. The ATP levels were determined 16 hpi using an ATP determination kit. Significant differences to the ATP level in VACV-infected cells without CCCP treatment defined by a P value <0.05 are indicated by asterisks. (F) Western blotting analysis of VACV protein expression with indicated treatment at 16 hpi using anti-VACV serum. The vertical lines in the VACV protein expression blot were generated due to a limitation of the Western blot imaging system when processing strong signals. (G and H) HeLa cells were infected with WRvFire VACV that contained a firefly luciferase gene under a viral early/late promoter with indicated treatment. Luciferase activities were measured at 2 hpi in the presence of AraC (G) or at 8

hpi (H) without AraC treatment. AraC is a DNA replication inhibitor that arrests VACV replication at the early gene expression stage. Significant differences to vehicle treatment defined by a P value <0.05 are indicated by asterisks.

Fig. 7. Short 5' UTRs of oxidative phosphorylation mRNAs can confer a translational advantage in VACV-infected cells. (A-B) Boxplots of the lengths (A) and normalized minimal free energy (MFE) (B) of oxidative phosphorylation and whole cellular mRNAs. *** indicates $p < 0.001$ using Mann-Whitney U test. (C) Relative luciferase activities of firefly reporter mRNAs under the control of various oxidative phosphorylation mRNA 5' UTRs in Mock- and VACV-infected cells. Transfection was carried out at 2 hpi and the luciferase activities were measured at 7 hpi. The number followed the gene name indicates the length of the 5' UTR. The firefly luciferase activities were normalized by a co-transfected renilla luciferase mRNA (transfection control). For each reporter mRNA, the luciferase activity in mock-infected cells was normalized as 1. Each result is an average of at least three independent experiments. The error bars indicate standard deviation. (D) Relative luciferase activities of firefly reporter mRNAs under the control of one copy or three tandem copies of Cox6A1 5' UTR in Mock- and VACV-infected cells. The experiment was carried out as in (C).

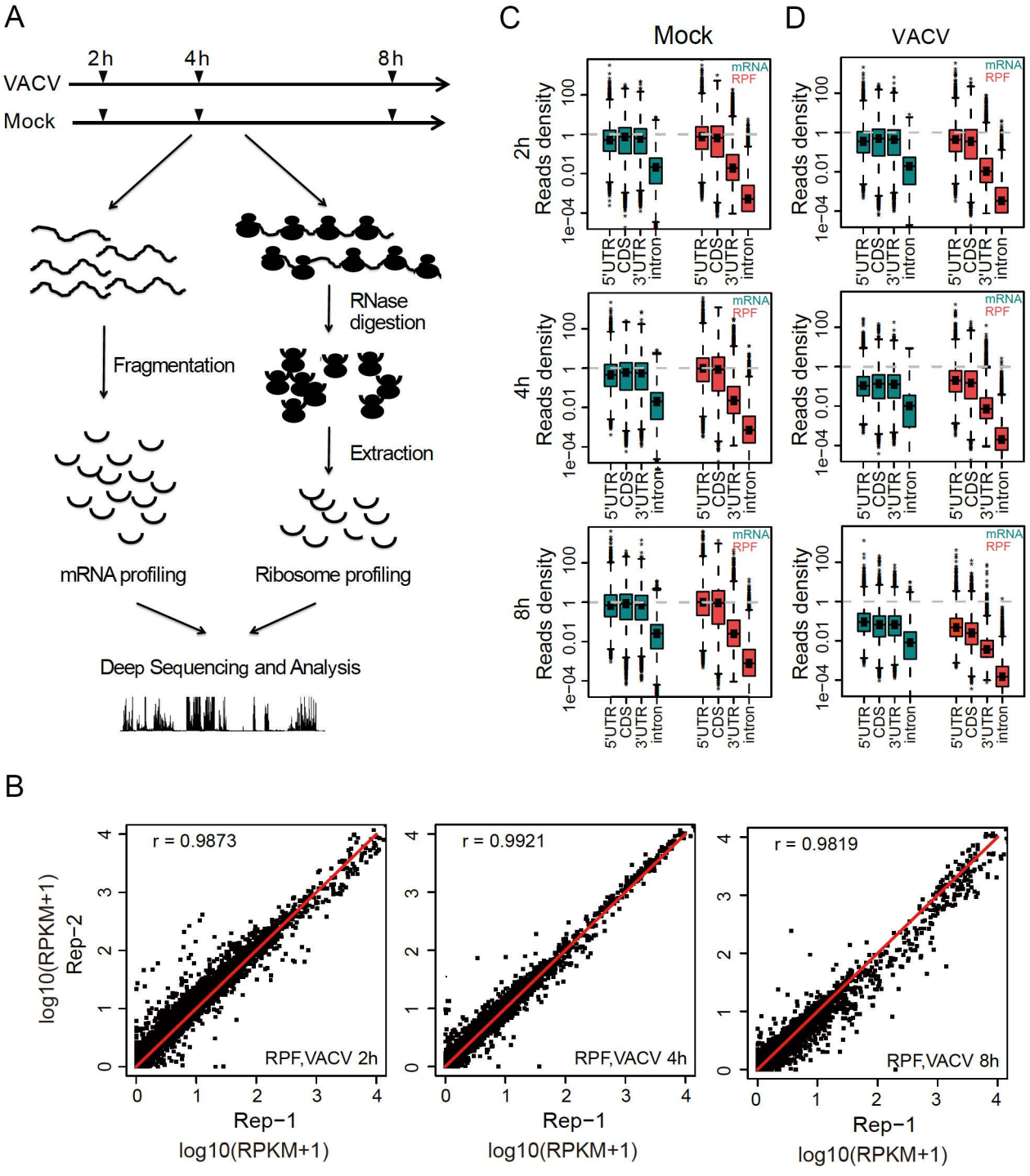

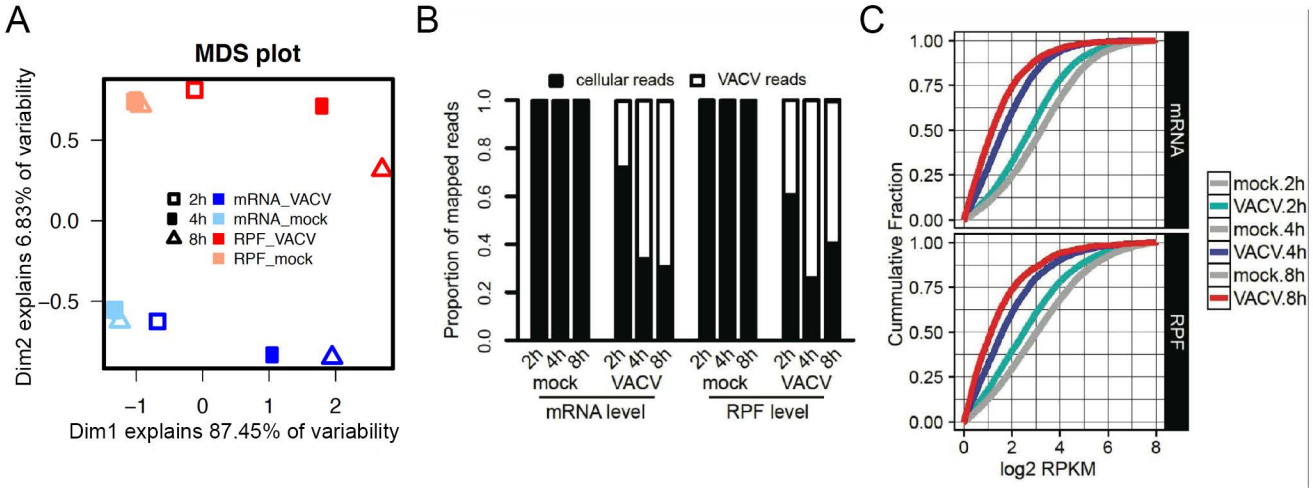

A

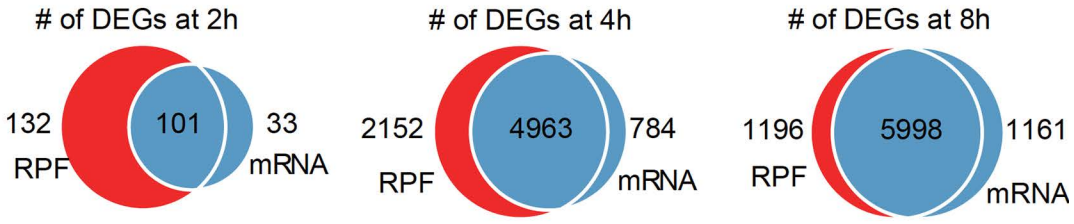

B

C

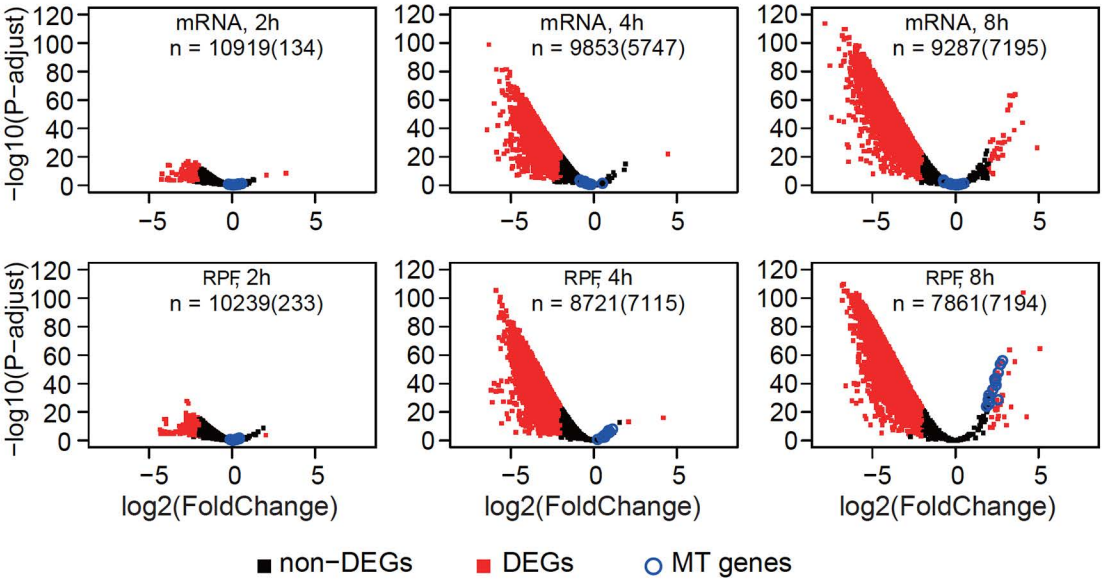

D

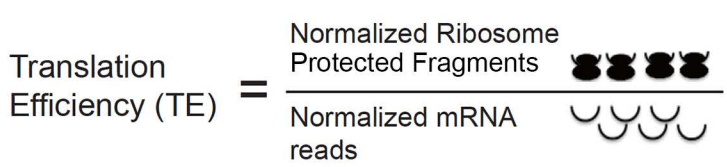

E

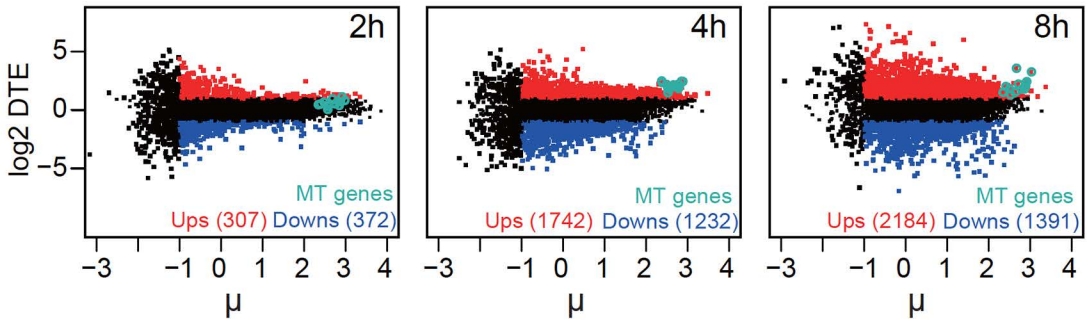

F

Pathway	P (adjusted)		
	2h	4h	8h
Ribosome	0.002	NS	NS
Oxidative phosphorylation	0.010	6.99E-09	0.042
Phenylalanine metabolism	NS	NS	0.042
Drug metabolism-cytochrome p450	NS	NS	0.042
Type I diabetes mellitus	NS	NS	0.042
Graft-versus-host disease	NS	NS	0.046

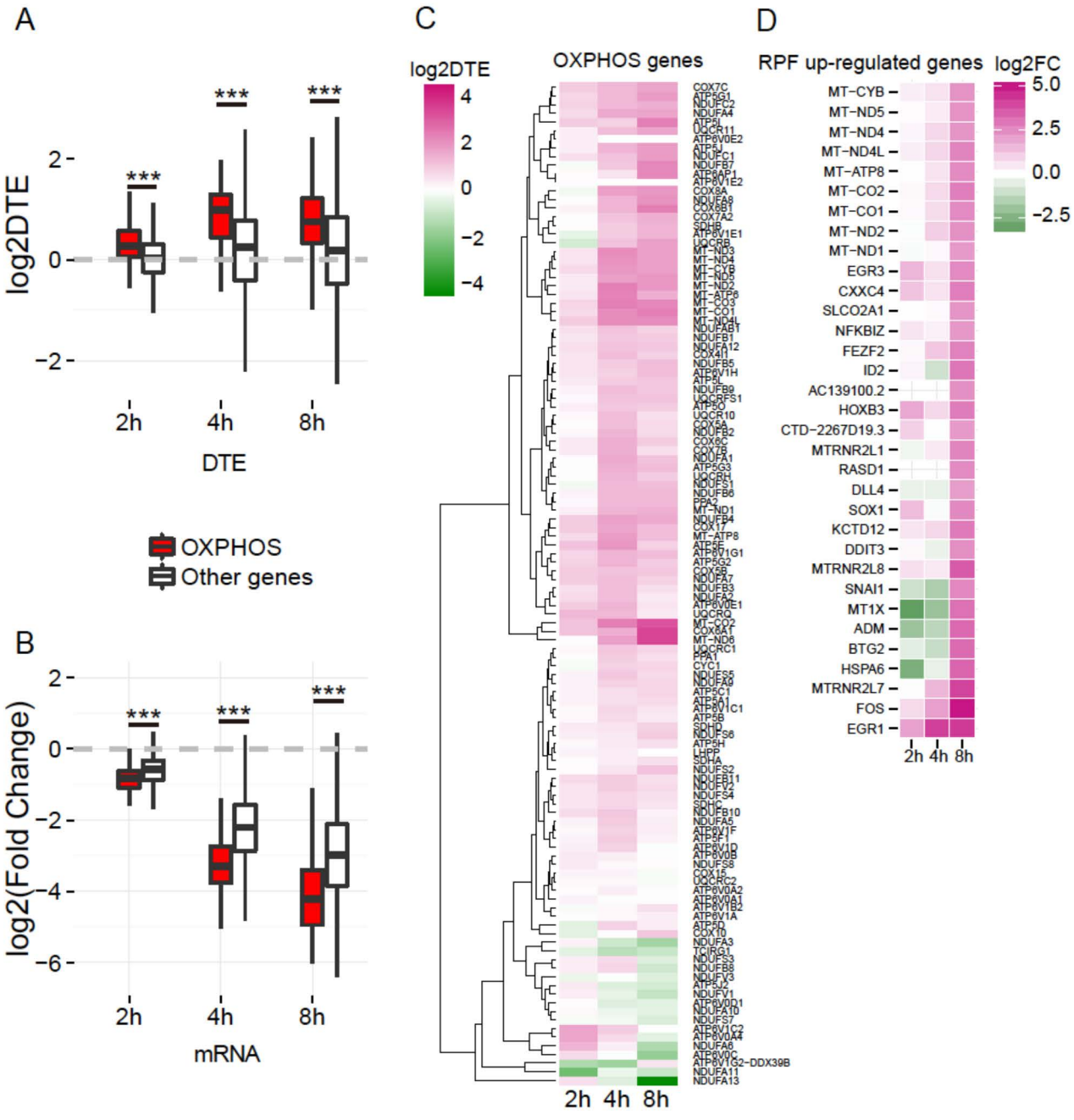

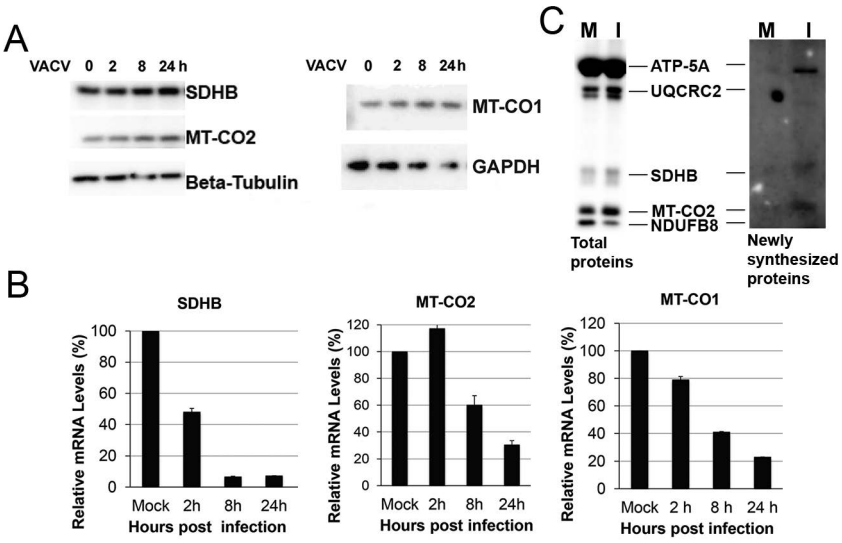

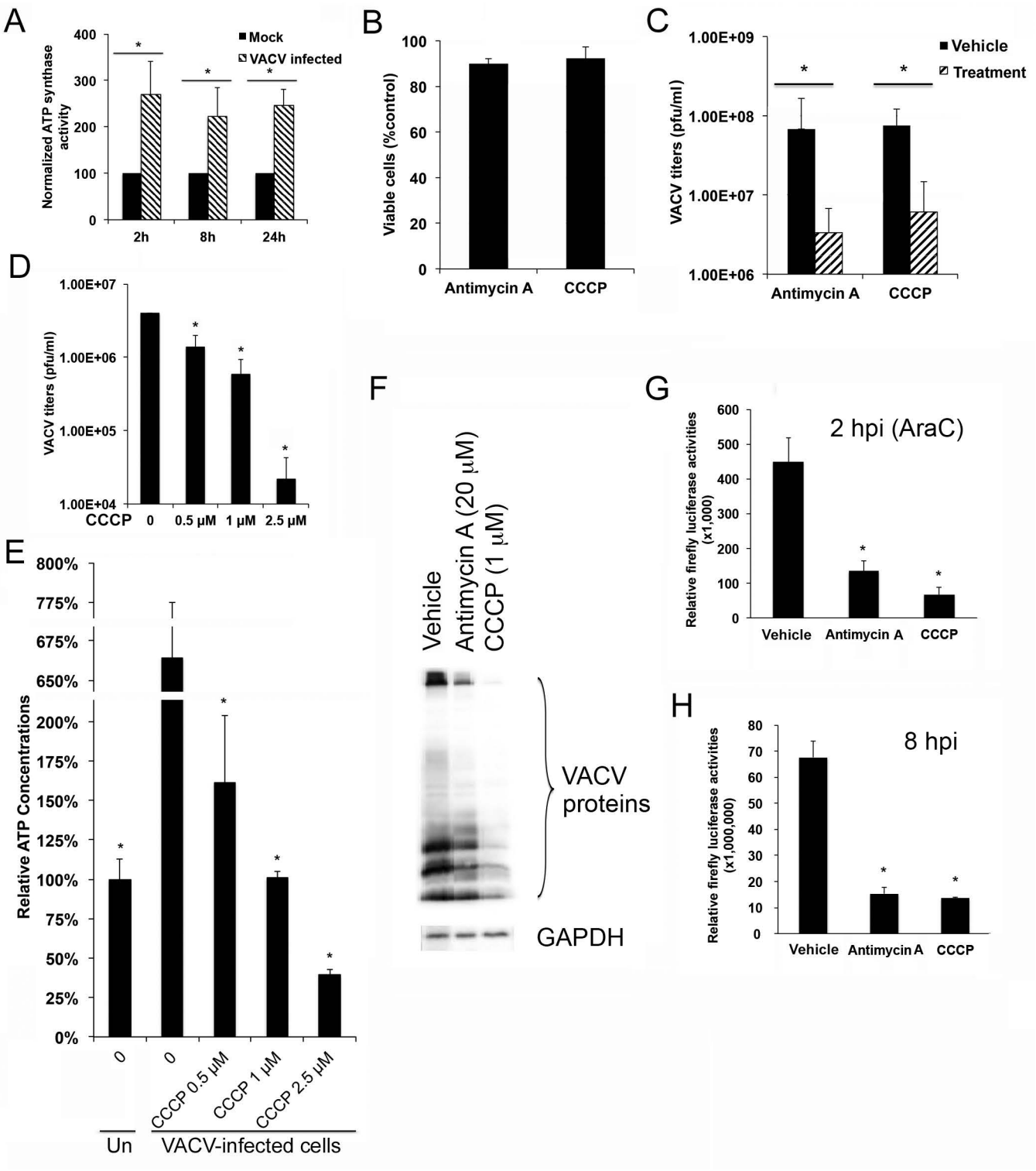

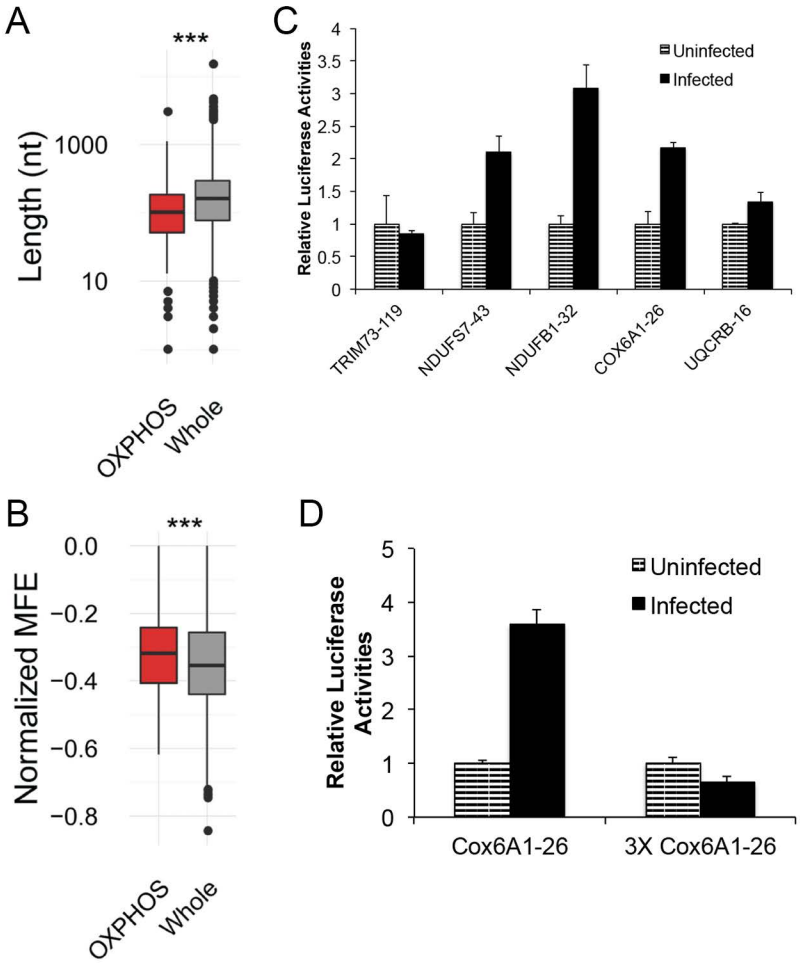

Journal of Virology